

DEPARTAMENT D' ASTRONOMIA I METEOROLOGIA



UNIVERSITAT DE BARCELONA



Near-relativistic electron events.  
Monte Carlo simulations of solar  
injection and interplanetary transport

Memòria presentada per  
**Neus Àgueda Costafreda**  
per optar al grau de Doctora  
per la Universitat de Barcelona.  
Barcelona, 20 de febrer de 2008



# 1 Introduction

## 1.1 Solar sources of near-relativistic electron events

Electrons at near-relativistic energies ( $E \geq 30$  keV, NR) are often observed as discrete events in the inner heliosphere following solar transient activity. Many NR electron events are temporally associated only with flares while others are associated with flares as well as with fast coronal mass ejections (CMEs) or with type II radio bursts<sup>1</sup>. Since CME onsets and associated flares can be simultaneous, distinguishing the sources of interplanetary NR electron events presents a serious challenge.

Wild et al. (1963) provided the first comprehensive picture of energetic electron production at the Sun. They deduced two separate phases of electron acceleration by combining radio, X-ray and H $\alpha$  flare observations. The first phase was a succession of bursts, each lasting  $\sim 1$  s, of  $\sim 100$  keV electrons that traveled upward through the corona to produce type III radio bursts<sup>1</sup>. In large flares, these energetic electrons were Fermi accelerated to higher ( $\leq 1$  GeV) energies in a second phase, due to traveling MHD shocks set up by the energy release of the first phase. As these shocks propagated away from the Sun, they were observed as slow frequency-drift type II radio bursts.

Although it was later recognized that ions could also be accelerated along with electrons in impulsive phases (Forrest & Chupp 1983), this two-class picture for solar electron acceleration has endured for several decades. Today we have far more extensive electron and other space observations to test and explore this relatively simple paradigm.

Nowadays we know that electrons and ions can be accelerated in solar flares (Hudson & Ryan 1995). The good correlation found between 4–8 MeV  $\gamma$ -ray-line and  $E > 50$  keV X-ray

---

<sup>1</sup>Electrons streaming through the solar corona produce an instability that results in plasma oscillations, also called Langmuir oscillations. These oscillations are converted into electromagnetic waves at the local electron plasma frequency and its second harmonic (Melrose 1985). The frequency of plasma oscillations depends on the density of the plasma ( $f \propto \sqrt{n}$ ). Therefore, as beams of electrons move to progressively lower coronal densities, the dynamic radio spectrum drifts to lower frequencies. Solar radio bursts are classified depending on their frequency drift. Type III radio bursts show a fast drift towards lower frequencies, implying a prompt release of electrons. Type II radio bursts show slower drifts towards lower frequencies and they are associated with electron beam distributions at coronal shocks.

fluences in solar flares suggests that the  $\sim 10$  MeV ions and the  $\sim 100$  keV electrons producing those emissions in the solar atmosphere are accelerated in a common process (Cliver et al. 1994). A similar correlation between the 2.22 MeV neutron-capture line and  $E > 300$  keV X-ray flare fluences in observations with the Ramaty High-Energy Solar Spectroscopic Imager (*RHESSI*) also indicates a common acceleration mechanism for  $E > 30$  MeV protons and  $E > 300$  keV electrons in flares (Shih et al. 2006). Solar flares are, therefore, obvious candidates for sources of the NR heliospheric electron events. The energy for electron acceleration in flares is presumed to arise in coronal flare magnetic reconnection (Hamilton et al. 2005). Flare electrons are assumed to be accelerated in a relatively confined region on relatively short time scales. The candidate mechanisms for flare acceleration have been reviewed by Bastian et al. (1998).

Electrons are also believed to be accelerated in much larger regions spanned by solar coronal shocks produced by CMEs moving at speeds higher than  $1000 \text{ km s}^{-1}$ , sufficient to exceed the local MHD fast-mode wave speeds (Mann et al. 2003). Recent work has shown that electron pitch-angle scattering at shock ripples with small scales can allow electron acceleration at quasi-perpendicular shocks (Burgess 2006), while at quasi-parallel shocks, energization can proceed by multiple shock encounters enabled by large-amplitude magnetic field fluctuations upstream of the shock (Mann et al. 2001).

## 1.2 Insights into solar sources from in-situ NR electron events

In-situ observations of NR electron events at 1 AU made by the *Interplanetary Monitoring Platform* (IMP) satellites in the period from 1966 September to 1967 December seemed to agree with the two phases of solar electron acceleration proposed by Wild et al. (1963). Lin (1970) distinguished two classes of  $E > 40$  keV electron events:

- “*Simple*” NR electron events with cutoff energies  $\leq 300$  keV, produced in small flares accompanied by type III, microwave and hard ( $\sim 20$  keV) X-ray bursts; and
- Proton-electron or “*complex*” events with relativistic electrons and energetic protons ( $E > 10$  MeV), produced in large eruptive flares accompanied by type II and type IV, intense microwave and hard X-ray bursts.

Simple NR electron events were associated with optical flares in the well connected W30 to W90 longitude range, and complex events were associated with flares located from E30 to W90.

With advances in the capabilities of charged-particle detectors, heliospheric electron events are now observed from the thermal solar-wind (Gosling et al. 2003) to the relativistic (Klassen et al. 2005) energy range. The observed velocity dispersions and antisunward flows establish that these electrons are generally accelerated in or near the solar corona.

Knowledge of the injection profile of NR electrons at the Sun is crucial when discerning the acceleration processes in action. The in-situ observations available to distinguish two, or more, kinds of sources of energetic electrons, however, are limited to the following: in-situ energy spectra, pitch-angle distributions (PADs), time-intensity profiles and the remotely observed solar coronal and interplanetary emissions associated with the coronal injections (e.g. X-ray emission, type III and II radio bursts). The analysis of such observations has suggested the following diagnostic methods to discern different kinds of solar sources from the observation of in-situ NR electrons:

- The inferred release time at the Sun deduced from the observed NR electrons at 1 AU has been compared with the timing of electromagnetic emissions (e.g. Kallenrode & Wibberenz 1991; Krucker et al. 1999; Haggerty & Roelof 2002).
- The measured spectral index of NR electron events observed at 1 AU has been used as an indicator of the source type (Simnett 2006).
- Multispacecraft observations have been used to yield the angular extents of events and their sources (Simnett 2003).
- Simulations of the interplanetary transport of NR electrons have been used to infer the injection profile of the source by comparing the simulations with in-situ observational data (Dröge et al. 2006; Wang et al. 2006; Maia et al. 2007; Agueda et al. 2008).

Unfortunately, the analysis of in-situ NR electron events poses difficulties due to

- the low sensitivity of the instruments. The low signal-to-noise ratio can mask part of the event and lead to a delay in the detection of the onset of the particle event (Sáiz et al. 2005).
- the incomplete pitch-angle coverage of the telescopes. The analysis of complete PADs, rather than only time-intensity profiles, is crucial for deriving the injection profile – otherwise, effects of prolonged injection cannot be separated from diffusive delays in the interplanetary medium.
- the uncertainties introduced at the very beginning of the event caused by instrumental effects, i.e. electron scattering out of the detector, which may result in some electrons depositing less than their total energy (Haggerty & Roelof 2003).

## 1 INTRODUCTION

- the location of the spacecrafts. Most of the observations come from spacecraft located at 1 AU, however, simultaneous in-situ measurements from more than one location would help to characterize the spatial and temporal variations of SEPs and the environment in which they propagate.

Moreover, there are unknown or poorly defined variables affecting the interpretation of

- the actual length and shape of the magnetic field line along which the electrons propagate,
- the conditions of interplanetary transport of the particles,
- the angular distance between the flare and the observer's magnetic footpoint (the observed particle event onset is more delayed with increasing angular distance; Kallenrode 1993).

### 1.3 Flare associations

Observations of 326 electron events with  $E > 2$  keV during a 15 months period in 1978–1979 by the *International Sun-Earth Explorer 3 (ISEE-3)* satellite at 1 AU showed that bursts of 2–100 keV electrons accelerated near the Sun were nearly always accompanied by solar type III radio bursts (Lin 1985).

Time-intensity observations of higher energy ( $E > 300$  keV) solar electron events from the *Helios* spacecraft showed that the electron injections at the Sun were also simultaneous with the onsets of the flare hard X-ray and microwave impulsive phases (Kallenrode & Wibberenz 1991). To derive the time of release of those particles observed at the onset of the event, Kallenrode & Wibberenz (1991) assumed scatter-free propagation. They calculated the release time by subtracting  $z/v$  to the in situ event onset time, where  $v$  is the particle velocity, and  $z$  is the path length along the Parker spiral magnetic field calculated from the ambient solar wind speed at the time of the onset. Using the same technique, Kallenrode & Svestka (1994) found good agreement between the onset of solar type III bursts and the inferred  $E > 300$  keV electron release times in an analysis of 27 electron events observed by the *Helios* spacecraft under solar minimum conditions, when the satellites were within 0.5 AU of the Sun.

The better time and energy resolution of the 3D Plasma and Energetic Particle (3DP) experiment (Lin et al. 1995), on board the *Wind* spacecraft, with respect to *ISEE-3*, allowed a more precise determination of the solar onset times. Krucker et al. (1999) used plots of

electron onset times versus  $c/v$  for their analysis, hereafter called  $c/v$  plots, where  $v$  is the electron speed and  $c$  is the speed of light. The  $c/v$  plots are based on two key assumptions

- the onset,  $t_r$ , of the solar particle injection profile is both impulsive and energy independent,
- the first particles observed at 1 AU propagate scatter-free, with pitch-angle cosines  $\mu \simeq 1$ , along a common travel path of distance  $D$  from the coronal injection site to the observer.

Under these assumptions,

$$t_0 = t_r + \frac{D}{v}. \quad (1.1)$$

where  $t_0$  is the onset time of the electron event at 1 AU. A plot of  $t_0$  against  $c/v$  for the first arriving particles yields a slope  $D/c$  and an intercept on the time axis at  $t_r$ . It is important to note that  $t_r$  is usually assumed to be only the beginning of an extended injection profile.

Krucker et al. (1999) applied the  $c/v$  plots to the study of 58 electron events observed at 1 AU by *Wind*/3DP. For energies lower than 25 keV, the lower signal-to-noise ratio of the telescope restricted the number of analyzed events to 12 of 58 events. Krucker et al. (1999) distinguished three different cases at low energies ( $< 25$  keV), see Figure 1.1: (1) In the most common case (7 of 12 events), a single straight line could fit the data over the entire inverse velocity range, and the determined release time was compatible with the release time of the type III radio burst ( $t_r \sim t_{\text{III}}$ ); (2) for three events, the data could also be fitted by a single line, but the determined electron release time was delayed relative to the type III start ( $t_r > t_{\text{III}}$ ); (3) in the two remaining events, low-energy electrons ( $< 25$  keV) were synchronous with the type III burst, but high-energy electrons ( $> 25$  keV) were delayed. Events with  $t_r \sim t_{\text{III}}$  were found to be well-connected with the approximated footpoint position, whereas the events that showed a delay ( $t_r > t_{\text{III}}$ ) occurred all far away from the footpoints of the nominal Parker spiral connecting the spacecraft with the Sun. At higher energies, the timing was different: in the majority of the cases (41 out of 58) the release times of the  $E > 25$  keV electrons were delayed up to half an hour from the preceding type III burst emission. This fact suggested that the low- and high-energy populations of interplanetary electron events do not originate from the same acceleration process.

The existence of a delay between the inferred release times of NR electrons and the preceding type III burst emission was later confirmed by Haggerty & Roelof (2002) using observations of 79 beamlike 38–315 keV electron events with the Electron, Proton, and Alpha Monitor (EPAM) on the *Advanced Composition Explorer* (ACE) spacecraft (Gold et al. 1998).

## 1 INTRODUCTION

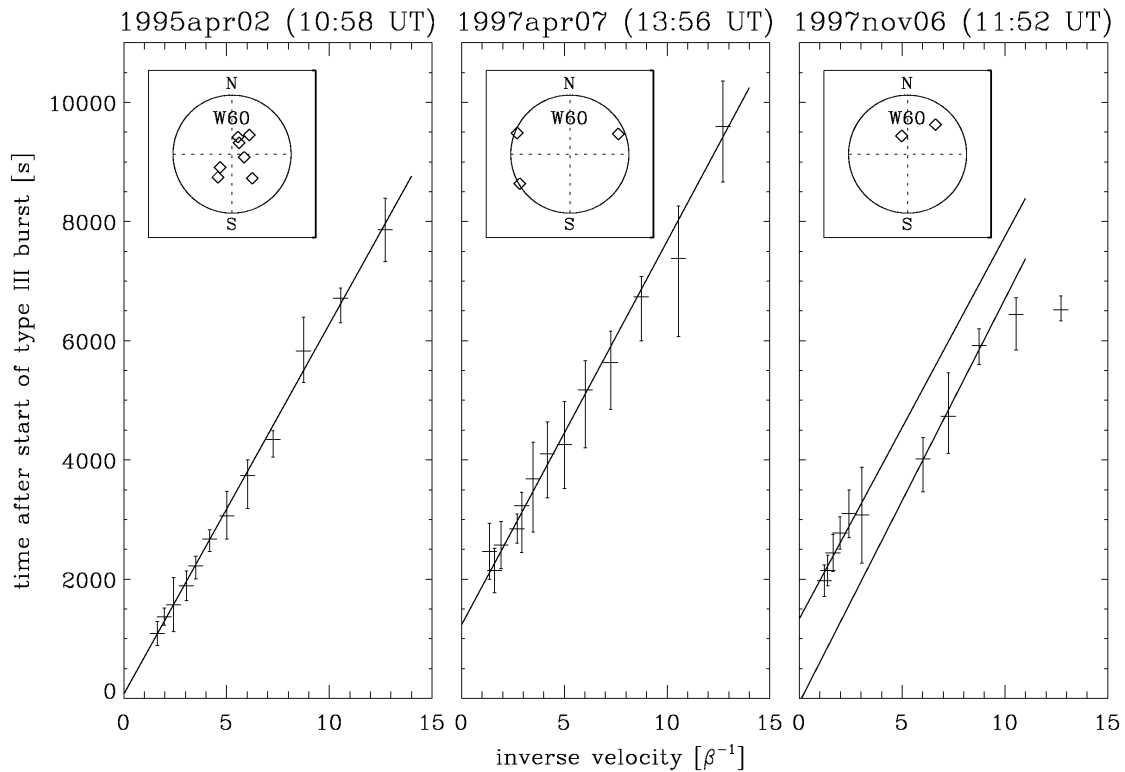


**Figure 1.1:** Onset time versus inverse velocity ( $\beta^{-1}$ ) plots for three electron events observed at 1 AU by Wind/3DP. The origin of the time axis corresponds to the start of the type III radio burst. The error bars show maximal uncertainties. The inserts show the flare locations relative to the footpoint of the Parker spiral for events belonging to the same class (from Krucker et al. 1999).

These authors assumed scatter-free electron propagation and fixed the length of the magnetic field line connecting the solar source with the spacecraft to 1.2 AU. The release times were then inferred by shifting the onset time of the event in the highest EPAM energy channel by 1.2 AU divided by the electron speed for that channel ( $v = 0.7c$ ). Figure 1.2 illustrates the observed delay for a representative NR electron event. Haggerty & Roelof (2002) found a median delay of 9.5 min between the metric type III bursts and the electron release times. The EPAM study was extended through 2002 March by Haggerty et al. (2003) in order to include 113 electron events. They found a median delay of 13 min between the metric type III bursts and the electron release times<sup>2</sup>.

Haggerty & Roelof (2002) also compared the timing of the electron release times to the start time of the electromagnetic ( $H\alpha$ , X-ray and microwave) emissions (see Figure 1.3) and found that the injection of the escaping NR electrons was delayed median time  $\sim 10$  min.

<sup>2</sup>Note, however, that the EPAM team identified a timing drift in the EPAM data in 2006. This timing drift was  $\sim 1$  min/year. The team identified the source of this drift, fixed the problem in the data and regenerated the entire EPAM dataset in January 2007. Therefore, the results obtained by Haggerty & Roelof (2002) and Haggerty et al. (2003) may vary with the timing correction. More details on the EPAM systematic timing problem can be found at the EPAM web site (<http://sd-www.jhuapl.edu/ACE/EPAM/EPAMtime.pdf>).



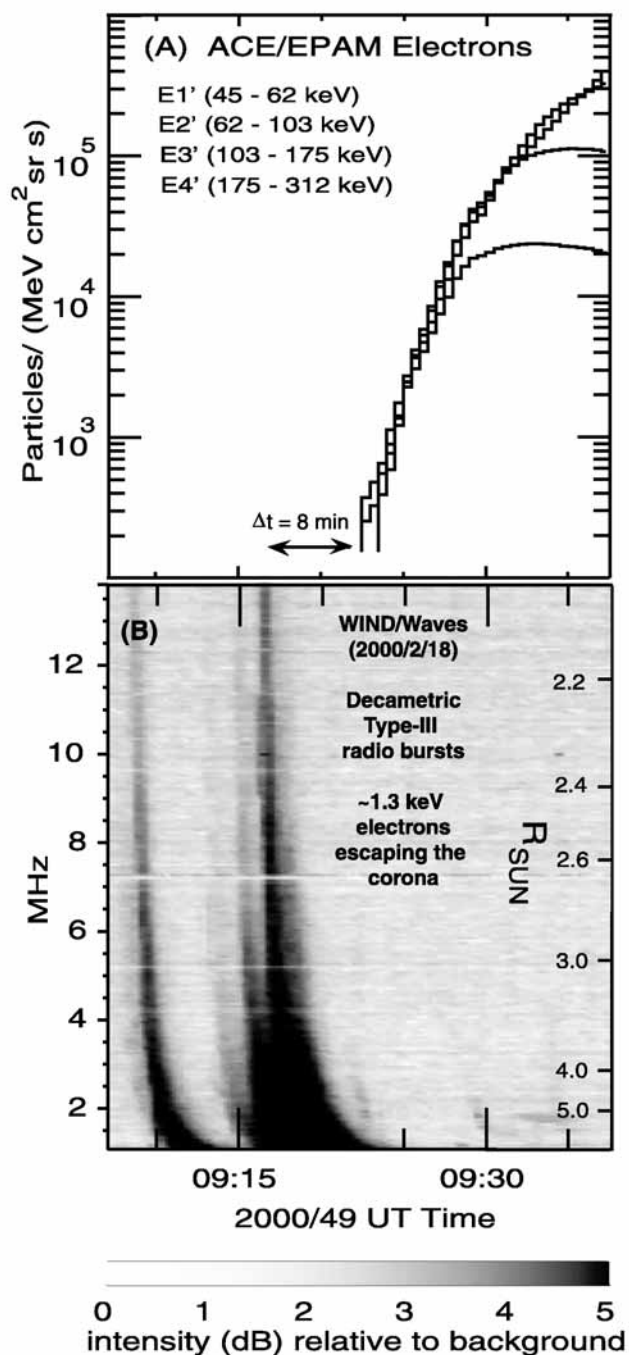


**Figure 1.2:** (A) Representative NR electron event with time taken back to the solar release time (assuming 1.2 AU propagation distance and  $v = 0.7c$ ) showing association with (B) type III radio bursts with time taken back (500 s) to coronal emission time. A delay is observed between the type III radio emission and the start of injection of the energetic electrons (from Haggerty & Roelof 2002).

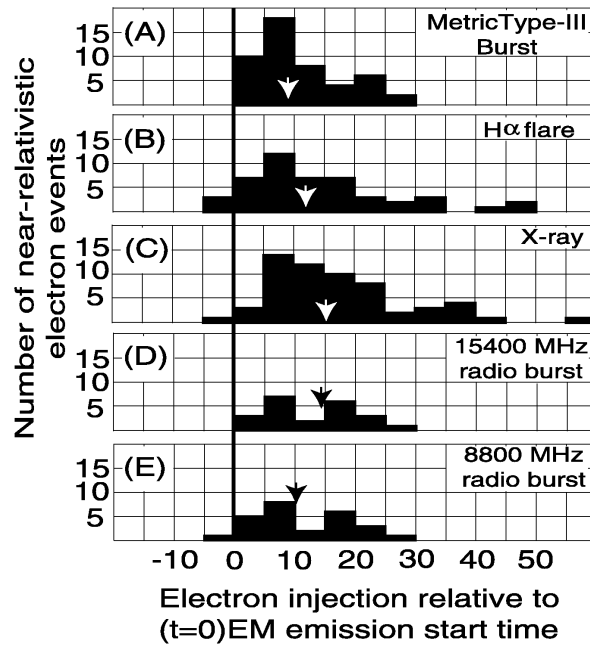


**Figure 1.3:** Timing delays between NR electron release time and start times of various electromagnetic emissions: (A) metric type III bursts, (B)  $H\alpha$  flares, (C) 1–8 Å soft X-ray, (D) 15400 MHz microwave burst, and (E) 8800 MHz microwave burst. Arrows indicate the median delay (from Haggerty & Roelof 2002).

These authors also studied the correlation of the peak intensities of NR electron events with the importance of the electromagnetic emissions of the associated flares. They found weak correlations with the microwave peak fluxes, soft X-ray peaks and soft X-ray fluences of the associated flares (the correlation coefficient,  $r$ , was smaller than 0.6 in the three cases). Thus, they dismissed the flare electromagnetic emissions as “only loosely related” to the electron intensities. Simnett et al. (2002) found slightly better correlation of peak electron intensities with CME speeds than with flare emissions and, therefore, suggested that the in-situ electrons and the electrons at the origin of type III emission belong to distinct populations, with the NR electrons accelerated at CME-driven shocks.

Nevertheless, studies comparing inferred solar release times of NR electrons with metric radio coronal imaging observations from the Nançay Radioheliograph provided an alternative explanation for the acceleration and release of electrons in some specific events. Maia & Pick (2004) and Klein et al. (2005) showed that electron release times closely coincide with the onset of, or changes seen in, long-duration radio emissions. This association supported a scenario in which the particles are accelerated at sites low in the corona, that originate in the wake of the magnetic restructuring linked to the CME development. Klein et al. (2005) studied the radio emission associated to 30 NR electron events observed by the *Wind*/3DP experiment. Although about a third of the events were associated with type II radio bursts,

Klein et al. (2005) argued that in most such cases the inferred electron injections were better matched to acceleration of radio-emitting electrons at heights lower than those of the shocks. In the same sense, Aurass et al. (2006) found evidence for several spatially distributed coronal magnetic field related acceleration sites in analyzing the high-energy particle acceleration and escape for the X-class flare of 2003 October 28.

Cane (2003) suggested a different explanation for the delays. She argued that NR electrons are injected at the time of the type III bursts and that the apparent delays are the result of propagation effects after injection. The supporting argument was the existence of a correlation between the injection delay times and the ambient solar wind densities observed at 1 AU. This result was also found by Kahler et al. (2007); but in addition, both the densities and the delay times were inversely correlated with solar wind speeds, suggesting that injection delays increase with longer travel distances, which result from decreasing solar wind speeds. Thus, Kahler et al. (2007) concluded that any NR electron onset delays due to a propagation effect are not necessarily due to enhanced ambient solar wind densities observed at 1 AU.

Wang et al. (2006) simulated three impulsive electron events observed by the *Wind*/3DP experiment from  $\sim 0.4$  to 300 keV by assuming interplanetary scatter-free propagation and triangular injections (with equal rise and fall times) at the Sun. Wang et al. (2006) found two distinct injections, one at low energies ( $\sim 0.4$  to 10 keV) starting  $9.1 \pm 4.7$  min before the start of the type III radio burst and lasting for 50–300 min; and a second at higher energies ( $> 15$  to 100 keV),  $7.6 \pm 1.3$  min after the start of the type III burst. Wang et al. (2006) concluded that low-energy electrons are likely to be the source of the type III radio bursts, whereas injection of high-energy electron occurs when the associated CME passes altitudes of  $\sim 1\text{--}6 R_{\odot}$ .

The origin of the delays observed between the inferred release times of NR electrons and the associated radio emissions is still under debate. Needless to say, future missions traveling close to the Sun, such as the *Heliophysical Explorers*<sup>3</sup> (*HELEX*) and *Solar Probe*<sup>4</sup> will help us to clarify the origin of such delays. To date, three mechanisms have been suggested to explain the delays:

1. Coronal shocks (observed as type II radio bursts) and/or by large-scale coronal EIT waves in conjunction with CMEs. The delays are due to either the acceleration time-scale or the time taken by the shock to establish magnetic connection with the observer.
2. Reconfiguration (reconnection) of the low corona behind the coronal shock/CME. In this approach, it is not until later in the solar event when NR electrons can escape into the interplanetary medium; the flare itself and the shock play a minor role.

---

<sup>3</sup>[http://lws.gsfc.nasa.gov/missions/sentinels/solar\\_sentinels\\_orbiter.htm](http://lws.gsfc.nasa.gov/missions/sentinels/solar_sentinels_orbiter.htm)

<sup>4</sup><http://solarprobe.gsfc.nasa.gov/>

3. Particle propagation effects across magnetic field lines. In this scenario, the type III radio emission and the in-situ electron event are produced by the same electron population, but particles arrive delayed at 1 AU due to their transport. In-situ observations closer to the Sun will confirm or rule out this possibility.

Given the rapid evolution in flare and CME activity at the onset of SEP events, a potential lack of accuracy in determining the particle release time can preclude reaching definitive conclusions about NR electrons origin. Therefore, it is important to note the limitations of the methods used to determine the electron release times. In the case of the  $c/v$  plots used by Krucker et al. (1999), numerical simulations (Lintunen & Vainio 2004; Sáiz et al. 2005) have shown that, in most cases, the onset times can align in nearly a straight line as a function of  $c/v$ . However, the estimated release times can be in error by several minutes, and the estimated path length can deviate greatly from the actual path length. Lintunen & Vainio (2004) concluded that the best timing results were obtained for events with interplanetary mean free paths  $\geq 0.3$  AU and clear intensity increases above the pre-event background. Sáiz et al. (2005) found that the error in the release time inferred from observations at 1 AU can vary from +6 to -9 min. The critical assumptions under  $c/v$  plots and some conflicting results from their use have been reviewed by Kahler & Ragot (2006). These authors warned that any insights into electron acceleration derived from comparisons of electron release times with solar phenomena may be compromised by spurious results of the  $c/v$  plot technique.

In the case of using the assumption of scatter-free propagation (Haggerty & Roelof 2002), the inferred electron release time may also be imprecise because of this limiting presupposition. In addition, the assumption that the length of the magnetic field line from the Sun to a near-Earth observer is 1.2 AU can be too restrictive because turbulent effects can lead to magnetic field-line lengths substantially longer than 1.2 AU (Ragot 2006).

### 1.4 Signatures of shock acceleration

Krucker et al. (1999) studied large-scale coronal disturbances observed by the Extreme Ultraviolet Imaging Telescope (EIT) on board *SOHO*, also known as EIT waves, in association with those events where the time of the type III burst and the inferred electron release time showed a delay. From the study, they concluded that some impulsive electron events were more likely related to propagating EIT waves than to the flare phenomenon itself. In addition, Krucker et al. (1999) suggested that fast moving wave fronts at high altitudes in the corona could link the flare site to the magnetic connection point to the Earth.

Later, Simnett et al. (2002) found correlations between CME velocities and electron prop-

erties such as intensities, hardness of spectra, and delays, and showed that the  $\sim 10$  min delays could be consistent with acceleration of the NR electrons by a shock driven by an outgoing CME. They noted that a coronal shock of  $\sim 1000 \text{ km s}^{-1}$ , forming in the low solar corona and propagating radially upward, takes 12 min to propagate  $1 R_{\odot}$ , at which point electrons could be accelerated by the shock to NR energies and reach open field lines. The prompt electromagnetic emissions (including the decametric type III bursts) would be then associated with the energy input that triggers the shock.

This scenario was supported by the results of Mann et al. (2003), who derived the existence of a local minimum of the Alfvén speed in the low corona, i.e.,  $1.2\text{--}1.8 R_{\odot}$ , and a broad maximum around  $2\text{--}6 R_{\odot}$ . Since shocks form more easily in regions with low Alfvén speed, a disturbance would need a period to travel from the flare or CME source site up to the local minimum Alfvén speed, where shock acceleration of electrons could occur (Mann et al. 2003).

Most of the electron events observed at 1 AU, however, have no associated shock signatures, suggesting a large population of electron events basically produced by flares. Moreover, for those electron events also associated with type II bursts and CMEs, it is difficult to distinguish between flare and shock sources. In the following sections, we review the techniques that have been applied to distinguish shock sources in NR electron events.

### 1.4.1 Solar type II burst associations

Solar type II radio bursts in the decametric-hectometric (DH) range are produced by CME-driven shocks, usually with speeds greater than  $500 \text{ km s}^{-1}$  (Gopalswamy et al. 2001, 2004). CMEs, flare ejecta, or flare blast waves have been related to the origin of metric type II burst shocks (Cliver et al. 1999; Gopalswamy et al. 2004). However, recent studies (Cliver et al. 2004; Cho et al. 2005; Shanmugaraju et al. 2006) support the view that CME drivers are the only metric and DH type II burst sources. Therefore shock acceleration of electrons can be tested by looking for associations of fast ( $\geq 1000 \text{ km s}^{-1}$ ) CMEs and/or solar type II radio bursts with electron events observed at 1 AU.

Simnett et al. (2002) examined transient coronal activity observed by LASCO around the release time inferred from NR electron ( $\sim 40\text{--}300 \text{ keV}$ ) events observed by ACE. They found that the NR electron release time was typically delayed by  $\sim 20$  min from the CME launch time and concluded that most of the NR electrons were produced in shocks driven by CMEs and released into space when the CMEs reached heights of  $1\text{--}2 R_{\odot}$  above the photosphere.

In an effort to verify this result, Kahler et al. (2005) examined the association of NR electron events with metric and DH type II bursts and CMEs. They showed that associations

between NR electron events and metric (37%) and DH (17%) type II bursts were not high. About 50% of the electron events were associated with CMEs sufficiently fast ( $> 900 \text{ km s}^{-1}$ ) and wide ( $> 60^\circ$ ) to drive shocks (Gopalswamy et al. 2001). Therefore, Kahler et al. (2005) concluded that the majority of the NR electron events do not originate in CME-driven shocks. This result was later supported by the statistical study of Simnett (2006).

Kahler et al. (2007) specifically compared type II event times and electron release times in order to determine whether or not electron injection occurred during the type II bursts themselves. Injection times were derived by subtracting from the apparent onset time the magnetic field path length (calculated from the ambient solar wind speed at the time of the onset) divided by the electron velocity. Almost half of the electron events were associated with metric or DH type II bursts, but most injections occurred before or after those bursts. They found that the electron release occurred during type II bursts in at most 17 of the 80 electron events.

### 1.4.2 Correlation between intensity peaks and CME speeds

Simnett et al. (2002) studied the correlation between peak intensities of NR electron events observed by EPAM and the speeds of the associated CMEs observed by LASCO. These authors found a positive correlation and concluded that it was consistent with electron acceleration at CME-driven shocks. This correlation appeared to improve with increasing electron energy, meaning that the effect was strongest for the electrons observed with highest energy. Note, however, that the correlation coefficients were small; Kahler et al. (2007) estimated them to be  $r \sim 0.57$ , whereas Simnett et al. (2002) did not provide them. Later, Haggerty et al. (2003) extended the study of Simnett et al. (2002) to more NR electron events observed by ACE and confirmed these results.

Nevertheless, in a similar study, Gopalswamy et al. (2004) found even lower correlations ( $r \sim 0.30\text{--}0.40$ ) for the peak intensities of 108 keV electron events observed by *Wind* versus the associated CME speeds.

### 1.4.3 Long-duration beam-like pitch-angle distributions

Kahler et al. (2007) compared the inferred release times of 80 NR electron events observed by *Wind* spacecraft with 40–800 MHz solar observations by the AIP radio telescope in Potsdam-Tremsdorf, Germany. Other than preceding type III bursts, they found no single radio signature characteristic of the inferred electron injection times. About half of the events were associated with metric or DH type II bursts, but most injections occurred before or after those

bursts. Kahler et al. (2007) also studied the approximate time over which the event PADs remained highly anisotropic, indicating a clear antisunward beaming of electrons. These times were obtained based on qualitative assessments of color-coded PADs of 82 keV electrons and ranged from 0.2 to 7 h. Kahler et al. (2007) found that electron events with long ( $\geq 2$  h) beaming times at 1 AU were well associated with type II bursts, which strongly supported the possibility of a class of shock-accelerated NR electron events.

#### 1.4.4 Spectral variations

Several authors have focused on the energy spectra to gain further understanding of the origin of the NR electrons observed at 1 AU. The underlying idea is that some of the spectral features of an event may reflect the acceleration and propagation history of the particles or even the superposition of solar sources.

The spectrum of differential intensities is usually characterized by a power law,  $dJ/dE \propto E^{-\gamma}$ . Normally, the differential intensity spectral index,  $\gamma$ , is computed by fitting a power-law to the maximum spin-averaged intensity observed by the telescope in each energy channel, within a given time period. Sometimes the energy spectrum displays breaks; in these cases, several spectral indices are used to describe the spectrum.

Lin et al. (1982) reported on nine large well-connected electron events<sup>5</sup> a characteristic double power law in energy between 20 keV and several MeV. When the fluxes were high enough, this spectrum was seen to extend to  $> 20$  MeV. They found a break in the spectra at 100–200 keV, in agreement with hard X-ray and microwave spectra, which suggested that the in-situ electrons were a representative sampling of the electron population at the Sun. Lin et al. (1982) found power law exponents of 0.6–2.0 below and 2.4–4.3 above the break.

Moses et al. (1989) compared soft X-ray flare durations with the spectrum of the associated electron events calculated in units of number density per momentum versus rigidity in the energy range between 75 keV and 100 MeV. Their study confirmed the double power-law shape with a break around 200 keV for events associated with short-duration soft X-ray emission ( $\leq 1$  h; SD) and that all events with long soft X-ray emission ( $> 1$  h; LD) exhibit a single power law in rigidity. Figure 1.4 shows the ratio between the low rigidity ( $E < 200$  keV) spectral index,  $\gamma_L$ , with respect to the high-rigidity ( $E > 200$  keV) spectral index,  $\gamma_H$ , as a function of the soft X-ray duration of the parent flare. It was remarkable that broken power-law spectra with steeper  $\gamma_L$  exponents and flatter  $\gamma_H$  exponents were associated exclusively with SD flares while single power-law spectra were associated preferentially with LD flares. Thus, a spectral distinction was sharply delineated at the flare duration of one hour. Moses

<sup>5</sup>Defined by flare locations between W30 and W90 solar longitude.

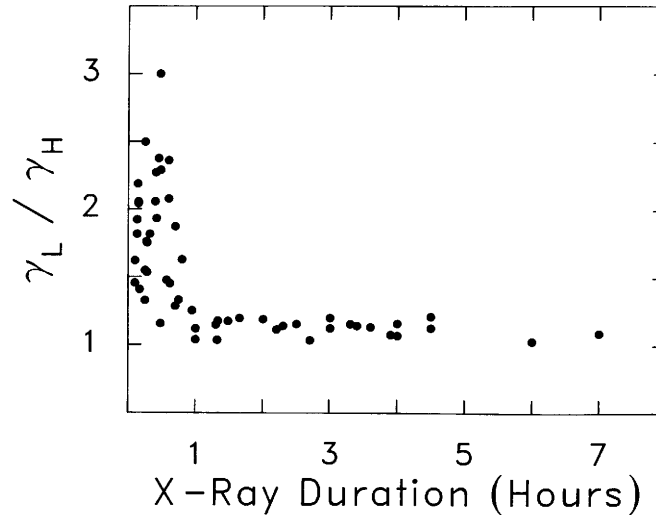


**Figure 1.4:** Ratio between the NR ( $E < 200$  keV) spectral index,  $\gamma_L$ , and the relativistic ( $E > 200$  keV) spectral index,  $\gamma_H$ , plotted against the soft X-ray duration; for 55 solar flares (from Moses et al. 1989).

et al. (1989) interpreted the two classes of electron spectra in terms of differences in coronal heights and densities for electron acceleration. They associated SD events with flares located low in the solar atmosphere (that is, in a dense environment where the effects of ionization energy losses on the acceleration process can not be ruled out), whereas LD events were attributed to acceleration high in the corona where these effects can be neglected. Nevertheless, Moses et al. (1989) also considered shock acceleration of electrons for LD events.

In a different approach, Simnett et al. (2002) studied the correlation between the power-law index of the electron spectrum as a function of energy for NR electron events observed by EPAM and the speeds of the associated CMEs observed by LASCO. These authors defined the spectral index as a function of the energy as the ratio of intensities measured in adjacent electron channels. Simnett et al. (2002) found that faster (slower) CMEs seemed to produce harder (softer) electron spectra<sup>6</sup>. Thus, they concluded that the spectral hardness of NR (38–315 keV) electrons was positively correlated with the CME speed. This result was consistent with the idea that faster CMEs could drive stronger shocks which could accelerate electrons to flatter energy spectra.

Simnett (2006) presented a survey of 45 of the most intense NR (40–300 keV) electron events observed by EPAM from September 1997 to September 2005 and found their spectral index to be between 1 and 3. He selected the most intense NR electron events based on the results from an earlier study (Simnett 2005b), where three discrete electron sources were distinguished for the 2003 October 28 electron event and the part of the event attributed

<sup>6</sup>Or, faster (slower) CMEs seemed to produce flatter (steeper) electron spectra.



to the flare itself was the one with the highest intensities (see section 1.5). Intense events were clearly distinguished from pulsed events by their higher peak intensities and longer timescales. Pulsed events were found to show spectral indices between 3.5 and 4.0 (Simnett 2006). Therefore, Simnett (2006) proposed to use the measured spectral index as an indicator of the source. He argued that electrons accelerated at flares may show low values of the spectral index (between 1 and 3), while electrons accelerated by CME-driven shocks may have a higher value (between 3.5 and 4.0). In the case of electrons coming from different solar sources, the measured spectrum would show an intermediate hardness, e.g.  $\sim 3.0\text{--}3.5$ .

### 1.4.5 Multispacecraft observations

Comparisons of NR electron event intensities observed by widely separated spacecraft can yield information about the role of shocks as electron accelerators, for example in broad shocks ( $\geq 100^\circ$ ). Simnett (2003) compared NR electron intensities on *ACE/EPAM* with those from the identical *HI-SCALE* instrument on the *Ulysses* spacecraft, from September 1997 to November 2000, when *Ulysses* was inbound from 5.4 to 2.2 AU and climbing from the ecliptic to  $80^\circ$  south heliographic latitude. Despite their large latitudinal and longitudinal separations, all NR electron events seen at *Ulysses* were also seen at *ACE* (see Figure 1.5). Most of the small electron events observed by *ACE*, however, did not appear at *Ulysses*. This could be due either to large radial gradients of the electron intensities that render them unobservable at *Ulysses* or, more likely, to the narrow source regions in solar flares where the particles in these events were injected. Large events, however, were observed simultaneously by *ACE* and *Ulysses*, regardless of their separation in the heliosphere. Therefore, the existence of these pairs of electron events observed at such different locations can be consistent with NR electron acceleration by CME-driven shocks.

MacLennan et al. (2003) extended the comparison of *ACE-Ulysses* observations of NR electrons through the *Ulysses* fast latitude scan (2000 November to 2001 October). These authors also observed electron events at all heliolatitudes, often being time-intensity profiles observed by *Ulysses* similar to those observed on *ACE* despite the significant latitudinal and radial separations of the two spacecraft.

## 1.5 Observation of two-phase electron events

If NR electrons can be accelerated by different physical processes near the Sun, we might expect to identify features of these processes in the time-intensity profiles of some of the NR electron events observed at 1 AU. The 2003 October 28 electron event has been well studied

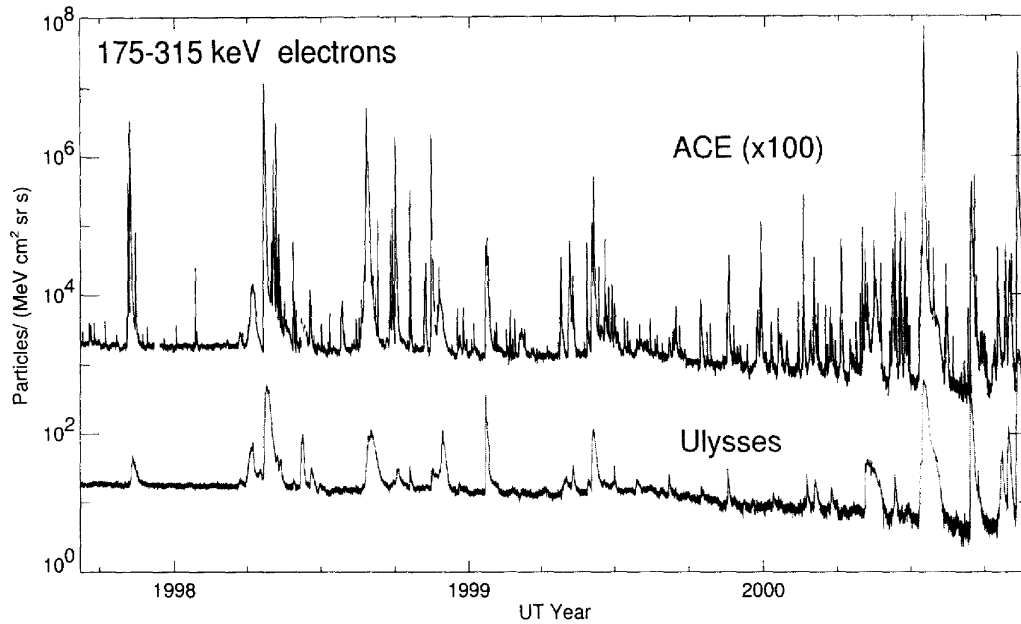


**Figure 1.5:** 175–315 keV electron intensities observed by ACE/EPAM ( $\times 100$ ) and Ulysses/HI-SCALE from 1997 September to 2000 November. At that time Ulysses was climbing from near the ecliptic to the heliographic latitude  $S80^\circ$  (from Simnett 2003).

by several authors (Klassen et al. 2005; Simnett 2005b; Miroshnichenko et al. 2005), as a good example of the manifestation of different types of solar acceleration mechanisms. The solar origin of this event was attributed to an X17.2/4B X-ray flare located in the active region NOAA 10486 at S16E08, slightly east of the central meridian, and a very fast ( $2459 \text{ km s}^{-1}$ ) halo CME (Klassen et al. 2005).

Klassen et al. (2005) distinguished two contributions in the in-situ time-intensity electron observations, both delayed relative to the electrons causing the type III radio bursts: (i) a symmetric 27–182 keV electron event of short duration ( $\sim 18$  min), showing significant velocity dispersion at the onset and delayed 11 min relative to the type III emission; and (ii) a weakly anisotropic 0.31–10.4 MeV electron event with a slow increase and a long duration ( $\sim 4$  hours), delayed relative to the type III emission by 25 min. Klassen et al. (2005) noted that the impulsive component injection occurred during decametric/metric type II and type IV bursts and, therefore, it could be attributed to either a shock or coronal magnetic field reconfigurations. These authors attributed the gradual component to magnetic reconfiguration behind the shock. Alternatively, Simnett (2005b) interpreted the impulsive component as a result of shock acceleration when the halo CME reached  $\sim 5R_\odot$  and attributed the gradual component to flare accelerated electrons gradually leaking out of a magnetic trap formed by the CME.

It was a challenge to understand how the flare electrons could be observed at Earth if

they were coming from a poorly connected region (S16E08). Miroshnichenko et al. (2005) noted that the dominant 164 MHz source during the type III bursts was located in the western hemisphere, well away from AR 10486. They suggested that the impulsive electrons were injected into a high-speed stream from the well-connected western source region, which also produced the earlier type III radio emission. These authors argued that the electrons of the gradual component were injected from the eastern flare site into the eastern footpoint of an interplanetary CME magnetic loop structure created by previous activity on the Sun and moved to 1 AU by that time.

Aurass et al. (2006) attributed the impulsive electrons to flare impulsive phase acceleration in a strong termination outflow shock located SW of AR 10486. These shocks occur in the upper and lower outflows of the reconnection region behind the CME and they may produce type II-like bursts with frequency drift rates implying very low ( $< 100 \text{ km s}^{-1}$ ) speeds (Aurass & Mann 2004). Aurass et al. (2006) attributed the source of the gradual electron event to the evolution of a large current sheet overlying the postflare loop system and excluded CME-driven shocks as a significant source of energetic electrons.

Kahler (2007) suggested that the impulsive component was produced in a well-connected flare region, and that the gradual electron component was produced in a CME-driven shock, based on its harder energy spectrum and longer timescale.

Thus, although they differed on the details, all these authors interpreted the 2003 October 28 electron event as at least two separate electron injections from different sources and/or acceleration mechanisms.

Simnett (2006) discussed another two-phase NR electron event observed by *ACE* on 2004 February 4. Figure 1.6 shows the spin-averaged 38–315 keV electron intensities observed by the LEFS60 and LEMS30 telescopes of the EPAM instrument on board *ACE* (see next chapter). The energy spectrum of the initial beamed pulse was relatively hard ( $\gamma = 2.5$ ) but softer than that of the gradual component ( $\gamma = 1.9$ ) (Simnett 2006). The lower panels in Figure 1.6 show the solar wind velocity, the IMF magnitude and direction ( $\theta$  is the latitude and  $\phi$  is the longitude, in the RTN spacecraft coordinate system). During the NR electron event *ACE* was embedded in a solar wind stream with a mean velocity  $554 \text{ km s}^{-1}$ . Both the solar wind velocity and the IMF direction were stable through the NR electron event. The nominal footpoint of the field line connecting *ACE* to the Sun was at a western longitude of  $43^\circ$ , as estimated from the observed solar wind speed. Simnett (2006) associated the origin of the NR electron event with a well-connected  $H\alpha$  flare at W48 and a slow ( $518 \text{ km s}^{-1}$ ) CME. The event therefore seemed consistent with a flare/shock two-injection scenario. Simnett (2006) preferred to associate the intense event with a flare and the pulsed event with a CME, but Kahler (2007) proposed the reverse association.

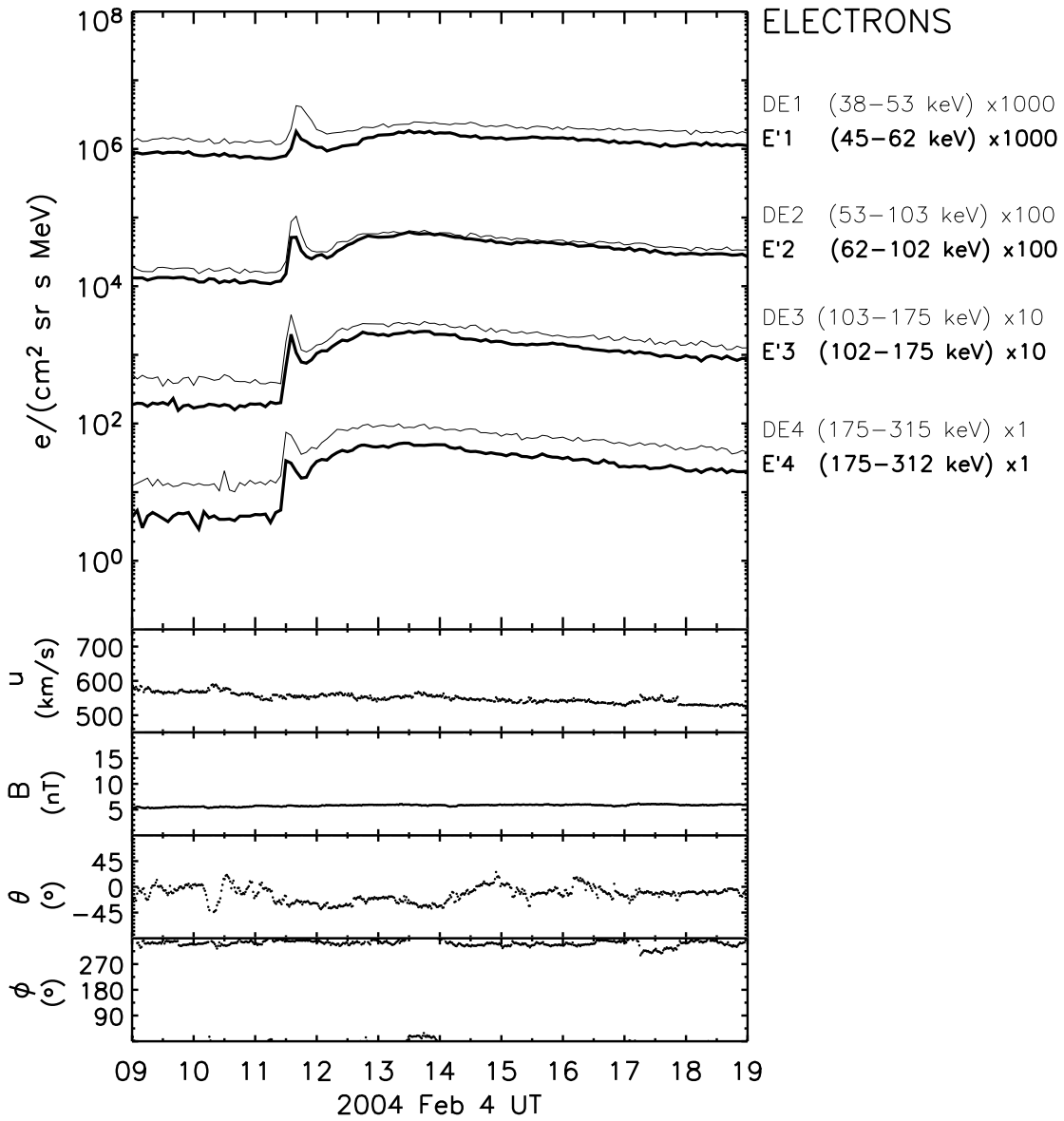


**Figure 1.6:** Two-phase NR electron event observed on 2004 February 4. From top to bottom: Electron spin-averaged intensities observed by the LEFS60 and the LEMS30 telescopes on board ACE. Solar wind velocity observed by ACE/SWEPAM. Magnetic field magnitude, latitude ( $\theta$ ) and longitude ( $\phi$ ) measured by the ACE/MAG experiment in the RTN coordinate system.

## 1.6 Aims of this thesis

The origin of intense NR electron events following transient solar activity have received large attention in the last four decades. The comparison of intensity profiles of NR electron events observed at 1 AU with flare signatures, CMEs and type II bursts, have suggested an important role for shock acceleration. Nevertheless, these observations have also indicated that perhaps most NR electron events observed at 1 AU are produced in flares (Kahler 2007). Recent work has established that

- There are many unresolved questions regarding the relative roles that flares and CME-driven shocks play in the acceleration and propagation of energetic particles from the solar corona into the interplanetary medium that need to be addressed.
- There are convincing cases that NR electron events seem to result solely from flares in the absence of either type II bursts or fast CMEs. Also, most NR electron events are not associated with metric or DH type II bursts (Kahler et al. 2007). Those events are therefore unlikely to be produced by coronal shocks. In other events CME-driven coronal shocks appear to be the only reasonable possibility based on the similarity of the time-intensity profiles to those of SEP events and on the extended longitudinal ranges of injection.
- Flare impulsive phases are often separated by only minutes from associated CMEs and type II bursts (Leblanc et al. 2001), so injection timings are a critical tool for associating electron populations with either flares or CME shocks.
- The solar release times must be correctly inferred before we can compare them with solar event phenomena.
- Events with double-phased time-intensity profiles (such as that of 2003 October 28) appear to be rare cases. If the two phases reflect separate flare and shock injections, it seems that only a single source, flare or shock, is dominant for the great majority of electron events.

Determining the solar origin of a given NR electron event remains a difficult task. However, several approaches have been proposed to resolve the solar sources of NR electron events. Accurate simulations of the transport of NR electrons are needed to reduce possible uncertainties in the source identification. Therefore, this thesis aims to provide

- a Monte Carlo code to simulate the interplanetary transport of NR electrons, in order to obtain the underlying injection profile close to the Sun, from the observation of in-situ NR electron events.

## 1 INTRODUCTION

- a detailed modelization of the sectorized NR electron measurements by the LEFS60 telescope of the EPAM experiment on board *ACE*, based on the calculation of the angular response function of the sectors.
- improved precision in the determination of the injection onset times. This determination will be much more reliable if it is based on a more complete treatment of interplanetary transport and observations.
- a comprehensive analysis of diverse NR electron events to determine the multitude of processes involved in the injection of solar NR electrons. Whereas the study of a specific event helps us to understand the underlying physics of the mechanisms involved in the generation of the particular event, it is necessary to extend the analysis to more than one event.
- a detailed survey of NR electron event spectra, intensities, timescales and source regions in order to provide useful information to gain understanding of the processes involved in the acceleration/injection of NR electrons.